Video Article

Sagittal Plane Kinematic Gait Analysis in C57BL/6 Mice Subjected to MOG35-55 Induced Experimental Autoimmune Encephalomyelitis

Maximillian DJ Fiander*[1], Matthew AJ Chedrawe*[1], Anna-Claire Lamport[1], Turgay Akay[2], George S Robertson[1,3]

[1]Pharmacology, Dalhousie University

[2]Medical Neuroscience, Dalhousie University

[3]Psychiatry, Dalhousie University

*These authors contributed equally

Correspondence to: Turgay Akay at Turgay.Akay@Dal.Ca, George S Robertson at robertgs@dal.ca

URL: https://www.jove.com/video/56032
DOI: doi:10.3791/56032

Keywords: Neurobiology, Issue 129, Kinematics, gait, experimental autoimmune encephalomyelitis, mouse, multiple sclerosis, motor deficits

Date Published: 11/4/2017

Citation: Fiander, M.D., Chedrawe, M.A., Lamport, A.C., Akay, T., Robertson, G.S. Sagittal Plane Kinematic Gait Analysis in C57BL/6 Mice Subjected to MOG35-55 Induced Experimental Autoimmune Encephalomyelitis. *J. Vis. Exp.* (129), e56032, doi:10.3791/56032 (2017).

Abstract

Kinematic gait analysis in the sagittal plane has frequently been used to characterize motor deficits in multiple sclerosis (MS). We describe the application of these techniques to identify gait deficits in a mouse model of MS, known as experimental autoimmune encephalomyelitis (EAE). Paralysis and motor deficits in mice subjected to EAE are typically assessed using a clinical scoring scale. However, this scale yields only ordinal data that provides little information about the precise nature of the motor deficits. EAE disease severity has also been assessed by rotarod performance, which provides a measure of general motor coordination. By contrast, kinematic gait analysis of the hind limb in the sagittal plane generates highly precise information about how movement is impaired. To perform this procedure, reflective markers are placed on a hind limb to detect joint movement while a mouse is walking on a treadmill. Motion analysis software is used to measure movement of the markers during walking. Kinematic gait parameters are then derived from the resultant data. We show how these gait parameters can be used to quantify impaired movements of the hip, knee, and ankle joints in EAE. These techniques may be used to better understand disease mechanisms and identify potential treatments for MS and other neurodegenerative disorders that impair mobility.

Video Link

The video component of this article can be found at https://www.jove.com/video/56032/

Introduction

Gait is a series of repetitive movements of the limbs used to achieve locomotion. Gait is comprised of step cycles, which are divided into two phases: the stance phase, which is when the foot is moving backwards on the ground to propel the body forwards; and the swing phase, where the foot is off the ground and moving forwards. Disturbances of gait are hallmark features of many neurodegenerative disorders, such as spinal cord injury (SCI), multiple sclerosis (MS), amyotrophic lateral sclerosis (ALS), Parkinson's disease (PD), and stroke; preclinical rodent models of these disorders often recapitulate their respective gait impairments[1]. The basic control mechanisms of locomotion in mice have been intensively studied[2,3]. Additionally, there are mouse models of many human neurological disorders[4]. Gait analysis in mice is therefore an attractive approach to measure multiple aspects of motor deficits that have known anatomical correlates. The study of gait in mouse models may provide insights into the neuropathological bases of locomotor deficits in neurodegenerative disorders, and enable the identification of potential treatments.

Some techniques that have been used to measure gait in rodents include visual inspection (*e.g.*, the Basso mouse scale[5] and open field test[6]) and analysis of gait from the ventral plane[7]. More recently, methods to measure sagittal plane kinematics of hindlimb movements have gained popularity because they provide more information about the execution of movement and consequently are more sensitive to subtle changes in gait[8,9,10,11]. Kinematic techniques developed to study hindlimb movement in sagittal plane while walking on a treadmill[9,12] have been extensively studied in the context of SCI, ALS, traumatic cortical injuries, stroke, and Huntington's disease[8,9,10,11,13,14,15,16]. In contrast, these techniques have seen limited use in the study of locomotor deficits for mouse models of multiple sclerosis[17].

Experimental autoimmune encephalomyelitis (EAE) is the most commonly used mouse model of MS[18]. The two main methods of inducing EAE is via active or passive inoculation. In active EAE, mice are immunized with myelin antigens, causing autoreactive T cell-mediated neuroinflammation and demyelination in the spinal cord and cerebellum. Passive EAE, on the other hand, is induced by transferring autoreactive T cells from a mouse with active EAE to a naïve mouse[19]. As described elsewhere, the disease course and neuropathology are influenced by the central nervous system (CNS) antigen and mouse strain[20,21,22,23,24,25]. In EAE experiments, control mice are injected with complete Freund's adjuvant (CFA) without the myelin antigen. EAE is characterized by ascending paralysis that begins with tail weakness and can potentially involve the forelimbs, resulting in ataxia and paralysis[20]. We have recently characterized gait changes in C57Bl/6 mice subjected to myelin oligodendrocyte glycoprotein 35-55 (MOG_{35-55})-induced EAE. These studies have shown gait analysis to be superior than classical behavioral analysis because deviations from normal ankle movement are highly correlated with the degree of white matter loss in the lumbar spinal cord of

EAE mice[26]. By contrast, the strength of the correlation between white matter loss and two other traditional behavioral measures (clinical scoring and rotarod) was much weaker[26].

We describe here the use of kinematic gait analysis to detect movement deficits in the sagittal plane of EAE mice walking on a treadmill. Five reflective markers were placed on a hindlimb to identify movement of the hip, knee, and ankle joints in high-speed video recordings. Motion analysis software was used to extract kinematic data about joint excursions. The utility of these techniques to quantify movement deficits for the MOG_{35-55} model of EAE are discussed. These techniques are also applicable to the study of gait deficits in other mouse models of neurodegenerative disorders.

Protocol

This protocol is in accordance with the Canadian Council on Animal Care guidelines and was approved by the Dalhousie University Committee on Laboratory Animals.

1. Construct Reflective Markers:

1. Using a hand-held hole punch, punch the desired number of small circles from a sheet of reflective paper. Each animal requires 5 markers for a single recording; two large and three small markers.
2. Using fine scissors, make a straight cut extending from the perimeter to the center of the circle.
3. Remove the paper backing of the marker to reveal the adhesive surface. Using fine forceps, grip the marker firmly and curl it in on itself using your finger to form a cone shape. To make a small marker, curl the cone tightly. To make a large marker, curl the cone loosely.
4. Using a hand-held glue gun, fill the inside of the cone-shaped marker with glue while gripping the tip of the cone with forceps and adhere the marker to a flat piece of cardboard. The glue will prevent the marker from collapsing and bending during recording to ensure optimal reflection of light. When the glue is dry (approximately 10 min), remove the marker from the cardboard with a scalpel (**Figure 1A**).

2. Prepare the Animal for Recording

1. Anesthetize the mouse with isoflurane gas (2.5%; 2 liters/min O_2) by placing the mouse into an induction chamber. Once the mouse is unconscious, place it into a nose cone positioned on top of a recirculating water heating blanket. The purpose of anesthetization is to immobilize the mouse for marker placement; the procedure is not painful. Therefore, depth of anesthesia does not need to be assessed.
2. Apply a topical eye lubricant to both eyes.
3. Shave the desired hindlimb using electric clippers. Begin at the ankle and extend to the spine and bottom of the ribs; ensure no fur is left as this will impair marker adhesion.
   Note: Here, the right hindlimb was recorded; however, either hindlimb can be used.
4. Using a permanent marker, indicate the location of the iliac crest and the hip joint. The iliac crest is just below the bottom of the ribs and is easily palpable by bringing the knees together under the mouse's body.
   Note: The hip joint can be found by flexing and extending the leg to find the articulation point between the pelvis and femur.
5. Using fine forceps, grasp the pointed end of a **small** marker and dip the base in fast-acting adhesive glue, or an equivalent alternative. Place the marker on the tip of the fourth digit and hold in place for 2-3 s to allow the glue to dry. Place the other two small markers on the metatarsophalangeal joint and ankle in the same manner (**Figure 1B**).
6. Place **large** markers on the iliac crest and hip joint (**Figure 1B**) in the same manner as the small markers.
7. Remove the mouse from the nose cone and immediately transfer to the recording room using a transfer cage. Place the mouse on the stationary treadmill and allow for full recovery from anesthesia.

3. Gait Recording

1. Prior to recording the mouse's gait, take a picture of a calibration block with known dimensions on the treadmill.
   Note: This will allow the pixels in the video to be converted to real measurements. The camera should be placed approximately 120 cm from the treadmill.
   1. Position the camera at the same height and level as the treadmill. Maintain the same camera position for the recordings following the calibration image.

2. Once the mouse has fully recovered from anesthesia, turn the treadmill to a low speed (5 cm/s) to let the mouse begin walking. Ensure that the treadmill belt direction is such that the markers on the mouse are facing towards the camera.
3. Increase the treadmill speed gradually up to 20 cm/s; this is the ideal speed for a consistent gait in most healthy mice.
   Note: Although it is ideal to have all mice walking at the same speed, some may be unable to consistently reach this speed.
   1. If the mouse is unable to walk at 20 cm/s, reduce the speed as necessary and be sure to make a note of this. Reduce the speed of the treadmill until consistent step cycles are achieved.
      Note: Later data analysis can adjust for differences in speeds.

4. Begin recording the video once the mouse is walking steadily (*i.e.*, walking at a consistent pace, not rearing or weaving side to side). Continue recording until 8 to 12 consecutive step cycles have been recorded. For every video, record the speed of the treadmill and the side of the mouse recorded.
5. Once recording is complete, turn off the treadmill and return the mouse to its cage. Clean the treadmill thoroughly between recordings as scents left behind by other mice may alter the behavior of incoming mice. To reduce stress and skin damage, do not remove the markers; allow the mice to remove them on their own.

4. Analysis

1. Process the videos using motion analysis software.
   Note: In our experiments, we used custom scripts designed for imaging and statistical software (see **Table of Materials**) that were written by Dr. Nicolas Stifani. The following steps are performed using the selected motion analysis software.
   1. Extract the pixel coordinates of the markers from the videos, and using the calibration video, transform the pixel values to centimeters and calculate the joint angles at each frame.
   2. Identify the beginning and end of each step cycle, thereby obtaining information about step duration and length.
   3. Normalize the step cycle duration to 200 normalized frames, such that swing and stance are represented by 100 frames, respectively.

2. Using the normalized frames, calculate kinematic parameters for data analysis using spreadsheet software (see **Table of Materials**).
   1. To establish the average angle of a particular joint, take the mean of all angles within a normalized frame as:
      $$Average\ angle = \frac{\sum_{i=1}^{n} x_i}{n}.$$
      Note: Here *x* represents the angle value at a given normalized frame, and *n* represents the normalized frame number.
   2. To establish the range of motion of a particular joint for a given mouse, subtract the smallest angle from the largest angle in a set of normalized frames as follows:
      $Range\ of\ motion = Angle_{maximum} - Angle_{minimum}$.
      Note: Here $Angle_{maximum}$ and $Angle_{minimum}$ are the greatest and smallest angles achieved within the normalized step cycle, respectively.
   3. To establish RMS difference, first subtract the average angle of each experimental time-point from the baseline recording. Next, square each difference, take the mean of all squared values and square root the mean. The equation is as follows:
      $$RMS\ difference = \sqrt{\frac{\sum_{i=1}^{n}(\bar{y}_i - y_i)^2}{n}}.$$
      Note: Here $\bar{y}$ represents the average angle from the baseline recording; *y* represents the average angle from each experimental time-point; *n* and represents the number of normalized frames. Root mean squared (RMS) difference is a measurement used to assess deviation in gait from baseline recordings.

3. Use scientific graphing and statistics software to analyze and present the data (see **Table of Materials**).

Representative Results

Figure 1 is a schematic representation of the procedure used for kinematic gait analysis. First, reflective markers are made and placed on a mouse at 5 anatomical points. Gait is then recorded while the mouse is walking on a treadmill. Motion analysis software is used to extract kinematic data for subsequent analysis.

Figure 2A-C represent the step cycle of a control CFA mouse for the hip, knee, and ankle joint angles recorded at three consecutive recording sessions spaced one week apart. The overlap between the waveforms shows minimal deviation in the step cycles from sessions 1-3. **Figure 2D-F** represent the step cycle of a second control CFA mouse that displayed greater walking variability from recording sessions 1-3. Although the step cycles are shifted along the y-axis, the shape of the waveforms remains consistent between recordings. This level of variability is typical for mouse walking.

Figure 3A-C represent the step cycle of a mouse with EAE recorded on three consecutive recording sessions. There are minimal changes in gait from the first to the second recording session, but by the third session, gait has been profoundly altered at all three joints. For the hip, a significant flattening over the step cycle has occurred, indicating a substantial loss of movement. The knee has become more flexed and less able to extend and support the animal's body weight. Movements at the ankle joint were also substantially altered. Foot dorsiflexion and plantar flexion are delayed during the swing (white panel) and stance (green panel) phases, respectively. These deficits are indicative of muscle weakness at this joint as the animal is impaired in its ability to both raise its foot during the swing phase, and propel the body forward during the stance phase.

The following data presented in **Figure 4** were republished from Fiander *et al.* (2017)[26] with permission. The data were analyzed using one-way repeated measures ANOVA with Holm-Sidak multiple comparisons test to compare all time points to baseline[26]. The average angle (**Figure 4A** and **Figure 4D**), range of motion (**Figure 4B** and **Figure 4E**) and RMS difference (**Figure 4C** and **Figure 4F**) were calculated at each time-point to quantify gait deficits (n=8 per group). In the present EAE experiment, the onset of clinical scores was DPI 14, which is after the second week of recording. CFA mice showed no change in average knee angle (**Figure 4A**) or knee RMS difference (**Figure 4C**), but did exhibit a small increase in knee range of motion [$F(2,7) = 5.871$, $p = 0.0083$], on both DPI 16 and 30 relative to the baseline (**Figure 4B**). This small change may reflect pain resulting from the CFA injection. In contrast to the CFA animals, there were large changes at the knee joint for EAE animals for the average angle [$F(6,7) = 11.08$, $p < 0.0001$] (**Figure 4D**), range of motion [$F(6,7) = 14.42$, $p < 0.0001$] (**Figure 4E**) and RMS difference (**Figure 4F**). The average angle was significantly reduced, indicating that EAE mice had their knees more flexed during walking. This may be indicative of muscle weakness, as the animals were unable to extend their knee joints to support their body weight. The range of motion was also decreased, again likely due to an inability of the animals to extend the knee joint. The significant increase in knee RMS difference indicates that the movements of the knee joint in EAE mice were substantially different from their baseline recording.

The data in **Figure 5** were analyzed using one-way repeated measures ANOVA with the Holm-Sidak multiple comparisons test that compared gait parameter values at clinical scores of 0.5 - 3.5 to those detected at a clinical score of 0. Correlational analysis was also performed using Spearman rho (ρ). The average knee angle (**Figure 5A**), range of motion (**Figure 5B**), and RMS difference (**Figure 5C**) were strongly correlated with clinical scores ($p < 0.001$). These correlations between joint movements and classical clinical scoring substantiate the validity of kinematic

gait analysis to assess motor deficits for EAE mice. Knee range of motion (**Figure 5A**) and RMS difference (**Figure 5C**) were significantly decreased beginning at a clinical score of 2.0 (p<0.05). These findings suggest that impaired knee movements do not contribute to motor deficits detected by clinical scores lower than 2.0. However, knee average angle (**Figure 5B**) was decreased beginning at a clinical score of 1.0 (p<0.05). This suggests that for knee movement, average angle is the most sensitive of the three measures.

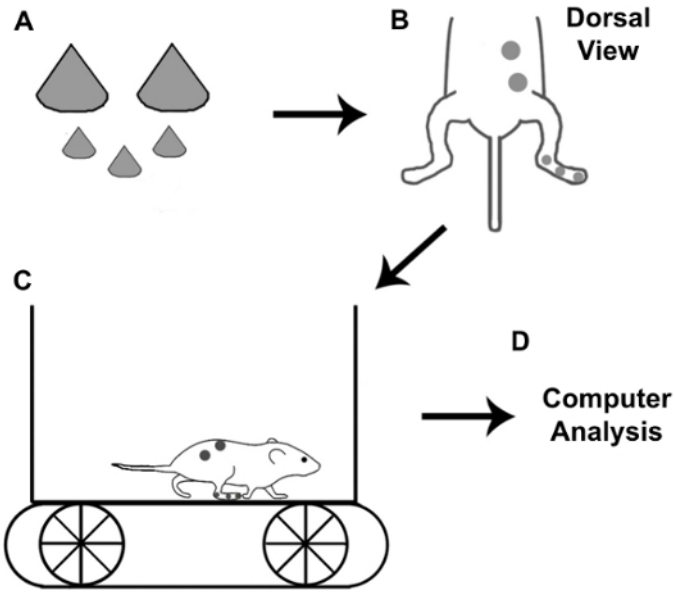

Figure 1: Schematic for kinematic gait recording with mice. Once reflective markers are made, they are placed on the iliac crest, hip joint, ankle, metatarsophalangeal joint, and the tip of the fourth digit. Gait is recorded by a high-speed camera while the mouse is walking on a treadmill. Motion analysis software is used to extract gait parameters for subsequent analysis. Please click here to view a larger version of this figure.

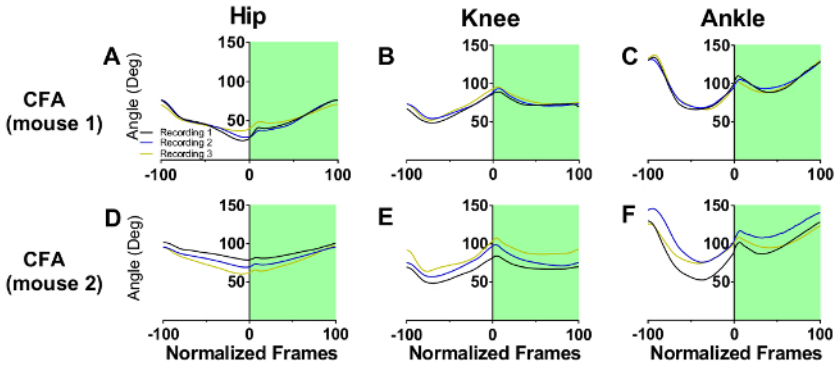

Figure 2: Example of step cycle waveforms in two control mice that received CFA
The white and green backgrounds represent the swing and stance phase, respectively. For mouse 1, the hip (**A**), knee (**B**), and ankle (**C**) step cycle waveforms overlap each other across 3 consecutive recording sessions spaced one week apart. For mouse 2, the hip (**D**), knee (**E**), and ankle (**F**) step cycle waveforms deviate slightly from each other due to the inherent variability in walking behavior. Please click here to view a larger version of this figure.

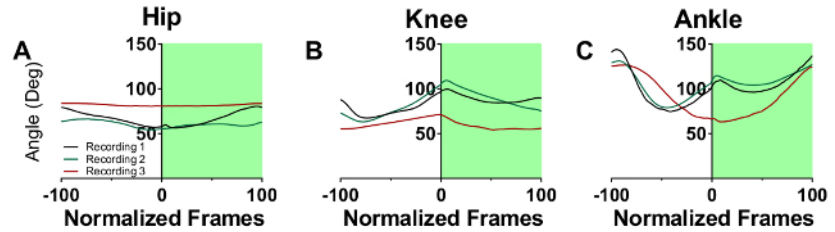

Figure 3: Step cycle waveforms in mice with EAE. The white and green backgrounds represent swing and stance phase, respectively, for three consecutive recording sessions spaced a week apart. By the 3rd recording session, the hip (**A**), knee (**B**), and ankle (**C**) waveforms are greatly changed due to EAE disease progression. Please click here to view a larger version of this figure.

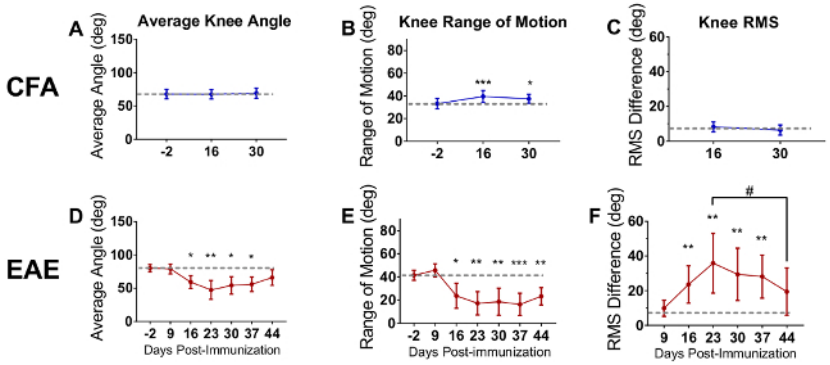

Figure 4: Average angle, range of motion, and root mean squared are used to analyze kinematic data. Average angle, range of motion, and RMS differences were calculated to quantify motor deficits in EAE mice. The average knee angle (**A**), range of motion (**B**), and RMS (**C**) for CFA mice remained relatively constant. Mice with EAE showed impaired knee average angle (**D**), range of motion (**E**), and RMS (**F**). Data are expressed as mean ± standard deviation; * $p<0.05$, ** $p<0.01$, *** $p<0.001$, difference from day post immunization (DPI) -2; # $p < 0.05$, difference from peak deficit. Reprinted from reference 26 with permission from original publishers. Please click here to view a larger version of this figure.

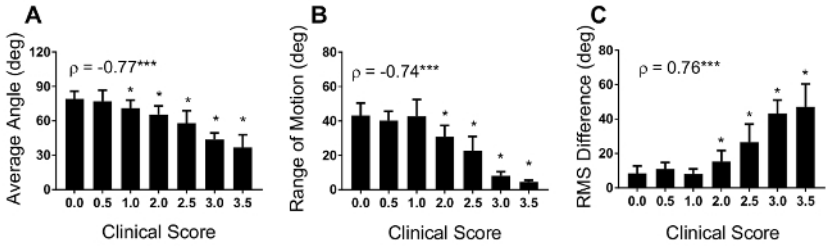

Figure 5. Average knee angle, range of motion and RMS difference correlate with clinical score
Correlation analysis was performed between three kinematic measures of knee movements and clinical scores to compare the two methods. The average knee angle (**A**), range of motion (**B**), and RMS difference (**C**) were strongly correlated with clinical scores. The knee range of motion and RMS difference decreased beginning at a clinical score of 2.0, while average knee angle was reduced earlier to a clinical score of 1.0. Data are expressed as mean ± standard deviation; * $p< 0.05$ difference from clinical score 0.0. For Spearman rho (ρ), *** $p< 0.001$. Please click here to view a larger version of this figure.

Discussion

In mice with EAE, the two most common methods of measuring motor deficits are clinical scoring and fall latency from a rotarod[27,28]. These techniques have several limitations. Although convenient and widely used, clinical scoring is limited by yielding only ordinal level data, meaning that the magnitude of the differences between clinical scores are not known. Clinical scoring also suffers from being unable to provide precise information about the nature of the motor deficits. The rotarod test improves on some limitations of clinical scoring, but only measures general motor coordination and does not measure specific aspects of walking.

By comparison, kinematic gait analysis provides sensitive measures about specific aspects of locomotion, including the range of motion and average angles at various joints. Subtle deficits in hip and knee joint movements for MOG_{35-55} EAE mice have been detected at DPI9, approximately 5-9 days before the onset of clinical symptoms or rotarod deficits[26]. These deficits persisted despite a complete remission of clinical signs and were observed in the absence of rotarod deficits[26]. Importantly, impaired ankle movements as measured by RMS difference correlated extremely well with white matter loss in the spinal cord[26].

Several methodological points deserve specific mention: 1) Accurate and consistent placement of the joint markers is crucial - the hip joint and iliac crest must be carefully identified by palpitation; 2) It is necessary to obtain recordings from 8-12 step cycles. Averaging these step cycles produces a representative average step cycle that can be further analyzed; 3) Optimal lighting conditions must be established to ensure that the markers are clearly visible in the recordings. If markers are not illuminated properly, this can make digitizing the videos a laborious process as many motion analysis programs will be unable to track the markers, necessitating manual tracking.

One additional limitation of this technique is that it is labor intensive. For example, to record and analyze data from a group of 10 mice, we estimate the total process takes approximately 7.0-9.0 hours (h). Making 50 markers (5 per mouse) takes about 2.0 h. Recording mouse walking behavior can be done either alone or in a pair. Working alone, it takes about 25 min per mouse, while working in a pair takes around 10 min per mouse; therefore, recording 10 mice may take from 1.5 h (pair) to 4.0 h (solo). Lastly, data analysis and graphing take approximately 3.5 h. Although this technique is labor intensive, we feel that the potential insights into disease mechanisms offered by kinematic gait analysis justifies this investment. Having good behavioral correlates of disease pathology is useful as serial measurements can be taken from a live mouse non-

invasively. Given the near perfect correlation between ankle kinematics and lumbar spinal cord white matter loss[26], this method may be used to ascertain the temporal profile of demyelination and remyelination in EAE mice over the course of an experiment, allowing recovery to be assessed.

Gait analysis is complicated by severe paralysis that restricts movement of the hindlimbs. However, even severely paralyzed mice (clinical score >3.0) are often able to ambulate to some extent. In these cases, the forelimbs are used to pull the animal forward, and some hindlimb movement occurs which can be measured by kinematic gait analysis. Even in these severe cases, it is still possible to measure recovery of hindlimb function over time. Only in very severe cases (20% of animals with clinical scores >3.5 at peak disease, DPI 16-23) have we been unable to obtain useful recordings of hindlimb movement. Nevertheless, these animals usually regain some hindlimb function by DPI 30, allowing meaningful recordings to be obtained at that time point.

A future application of this technique is coupling kinematic data with simultaneous electromyographic recordings of the hindlimb during locomotion. This technique has been done in mouse models of ALS and SCI and can be used to elucidate the relationship between muscle activity, innervation, and gait. This technique could also be coupled with more targeted models of MS and demyelination that may produce more discrete gait deficits, including focal EAE models[29,30] or cuprizone-induced demyelination[31].

The techniques we have described for the measurement of joint movements in EAE mice can also be applied to other disorders that impair gait. Distinct changes in gait have been reported for mouse models of PD, SCI, ALS, and stroke[8,9,10,11,13,14]. For example, rodent models of PD are characterized by reduced stride length and velocity, resulting in elevated cadence to maintain walking speed[32]. Kinematic gait analysis therefore provides powerful behavioral tools to elucidate disease mechanisms and identify potential treatments using these models.

Disclosures

The authors declare that they have nothing to disclose.

Acknowledgements

We would like to acknowledge Sid Chedrawe for his technical assistance with filming. This work was supported by funding from the MS Society of Canada (EGID 2983).

References

1. Giladi, N., Horak, F. B., & Hausdorff, J. M. Classification of gait disturbances: distinguishing between continuous and episodic changes. *Mov Disord.* **28** (11), 1469-1473 (2013).
2. Kiehn, O. Decoding the organization of spinal circuits that control locomotion. *Nat Rev Neurosci.* **17** (4), 224-238 (2016).
3. Akay, T., Tourtellotte, W. G., Arber, S., & Jessell, T. M. Degradation of mouse locomotor pattern in the absence of proprioceptive sensory feedback. *Proc Natl Acad Sci U S A.* **111** (47), 16877-16882 (2014).
4. Hafezparast, M., Ahmad-Annuar, A., Wood, N. W., Tabrizi, S. J., & Fisher, E. M. Mouse models for neurological disease. *Lancet Neurol.* **1** (4), 215-224 (2002).
5. Basso, D. M. *et al.* Basso Mouse Scale for locomotion detects differences in recovery after spinal cord injury in five common mouse strains. *J Neurotrauma.* **23** (5), 635-659 (2006).
6. Tatem, K. S. *et al.* Behavioral and locomotor measurements using an open field activity monitoring system for skeletal muscle diseases. *J Vis Exp.* (91), e51785 (2014).
7. Hetze, S., Romer, C., Teufelhart, C., Meisel, A., & Engel, O. Gait analysis as a method for assessing neurological outcome in a mouse model of stroke. *J Neurosci Methods.* **206** (1), 7-14 (2012).
8. Preisig, D. F. *et al.* High-speed video gait analysis reveals early and characteristic locomotor phenotypes in mouse models of neurodegenerative movement disorders. *Behav Brain Res.* **311** 340-353 (2016).
9. Leblond, H., L'Esperance, M., Orsal, D., & Rossignol, S. Treadmill locomotion in the intact and spinal mouse. *J Neurosci.* **23** (36), 11411-11419 (2003).
10. Ueno, M., & Yamashita, T. Kinematic analyses reveal impaired locomotion following injury of the motor cortex in mice. *Exp Neurol.* **230** (2), 280-290 (2011).
11. Zorner, B. *et al.* Profiling locomotor recovery: comprehensive quantification of impairments after CNS damage in rodents. *Nat Methods.* **7** (9), 701-708 (2010).
12. Pearson, K. G., Acharya, H., & Fouad, K. A new electrode configuration for recording electromyographic activity in behaving mice. *J Neurosci Methods.* **148** (1), 36-42 (2005).
13. Balkaya, M., Krober, J. M., Rex, A., & Endres, M. Assessing post-stroke behavior in mouse models of focal ischemia. *J Cereb Blood Flow Metab.* **33** (3), 330-338 (2013).
14. Akay, T. Long-term measurement of muscle denervation and locomotor behavior in individual wild-type and ALS model mice. *J Neurophysiol.* **111** (3), 694-703 (2014).
15. Taylor, T. N., Greene, J. G., & Miller, G. W. Behavioral phenotyping of mouse models of Parkinson's disease. *Behav Brain Res.* **211** (1), 1-10 (2010).
16. Chen, K. *et al.* Differential Histopathological and Behavioral Outcomes Eight Weeks after Rat Spinal Cord Injury by Contusion, Dislocation, and Distraction Mechanisms. *J Neurotrauma.* **33** (18), 1667-1684 (2016).
17. de Bruin, N. M. *et al.* Multiple rodent models and behavioral measures reveal unexpected responses to FTY720 and DMF in experimental autoimmune encephalomyelitis. *Behav Brain Res.* **300** 160-174 (2016).
18. Steinman, L., & Zamvil, S. S. How to successfully apply animal studies in experimental allergic encephalomyelitis to research on multiple sclerosis. *Ann Neurol.* **60** (1), 12-21 (2006).

19. Emerson, M. R., Gallagher, R. J., Marquis, J. G., & LeVine, S. M. Enhancing the ability of experimental autoimmune encephalomyelitis to serve as a more rigorous model of multiple sclerosis through refinement of the experimental design. *Comp Med.* **59** (2), 112-128 (2009).
20. Bittner, S., Afzali, A. M., Wiendl, H., & Meuth, S. G. Myelin oligodendrocyte glycoprotein (MOG35-55) induced experimental autoimmune encephalomyelitis (EAE) in C57BL/6 mice. *J Vis Exp.* (86) (2014).
21. Beeton, C., Garcia, A., & Chandy, K. G. Induction and clinical scoring of chronic-relapsing experimental autoimmune encephalomyelitis. *J Vis Exp.* (5), e224 (2007).
22. Barthelmes, J. *et al.* Induction of Experimental Autoimmune Encephalomyelitis in Mice and Evaluation of the Disease-dependent Distribution of Immune Cells in Various Tissues. *J Vis Exp.* (111) (2016).
23. Shaw, M. K., Zhao, X. Q., & Tse, H. Y. Overcoming unresponsiveness in experimental autoimmune encephalomyelitis (EAE) resistant mouse strains by adoptive transfer and antigenic challenge. *J Vis Exp.* (62), e3778 (2012).
24. Stromnes, I. M., & Goverman, J. M. Passive induction of experimental allergic encephalomyelitis. *Nat Protoc.* **1** (4), 1952-1960 (2006).
25. Stromnes, I. M., & Goverman, J. M. Active induction of experimental allergic encephalomyelitis. *Nat Protoc.* **1** (4), 1810-1819 (2006).
26. Fiander, M. D., Stifani, N., Nichols, M., Akay, T., & Robertson, G. S. Kinematic gait parameters are highly sensitive measures of motor deficits and spinal cord injury in mice subjected to experimental autoimmune encephalomyelitis. *Behav Brain Res.* **317** 95-108 (2017).
27. Jones, M. V. *et al.* Behavioral and pathological outcomes in MOG 35-55 experimental autoimmune encephalomyelitis. *J Neuroimmunol.* **199** (1-2), 83-93 (2008).
28. van den Berg, R., Laman, J. D., van Meurs, M., Hintzen, R. Q., & Hoogenraad, C. C. Rotarod motor performance and advanced spinal cord lesion image analysis refine assessment of neurodegeneration in experimental autoimmune encephalomyelitis. *J Neurosci Methods.* **262** 66-76 (2016).
29. Sasaki, M., Lankford, K. L., Brown, R. J., Ruddle, N. H., & Kocsis, J. D. Focal experimental autoimmune encephalomyelitis in the Lewis rat induced by immunization with myelin oligodendrocyte glycoprotein and intraspinal injection of vascular endothelial growth factor. *Glia.* **58** (13), 1523-1531 (2010).
30. Merkler, D., Ernsting, T., Kerschensteiner, M., Bruck, W., & Stadelmann, C. A new focal EAE model of cortical demyelination: multiple sclerosis-like lesions with rapid resolution of inflammation and extensive remyelination. *Brain.* **129** (Pt 8), 1972-1983 (2006).
31. Franco-Pons, N., Torrente, M., Colomina, M. T., & Vilella, E. Behavioral deficits in the cuprizone-induced murine model of demyelination/remyelination. *Toxicol Lett.* **169** (3), 205-213 (2007).
32. Goldberg, N. R., Hampton, T., McCue, S., Kale, A., & Meshul, C. K. Profiling changes in gait dynamics resulting from progressive 1-methyl-4-phenyl-1,2,3,6-tetrahydropyridine-induced nigrostriatal lesioning. *J Neurosci Res.* **89** (10), 1698-1706 (2011).

